AMERICAN UNIVERSITY OF BEIRUT

HUMIDITY CONTROL IN A SPACE CONDITIONED BY A LIQUID DESICCANT MEMBRANE CHILLED CEILING WITH DISPLACEMENT VENTILATION SYSTEM

by
RACHA YOUSSEF SEBLANY

A thesis
submitted in partial fulfillment of the requirements
for the degree of Master of Engineering
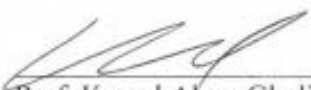to the Department of Mechanical Engineering

AMERICAN UNIVERSITY OF BEIRUT

HUMIDITY CONTROL IN A SPACE CONDITIONED BY A LIQUID DESICCANT MEMBRANE CHILLED CEILING WITH DISPLACEMENT VENTILATION SYSTEM
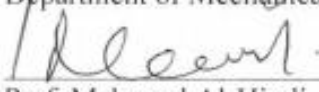
by
RACHA YOUSSEF SEBLANY

Approved by:

_____

Prof. Nesreen Ghaddar, PhD, Professor   Co-Advisor
Department of Mechanical Engineering

_____

Prof. Kamel Abou Ghali, PhD, Professor   Co-Advisor
Department of Mechanical Engineering

_____

Prof. Fadl Moukalled, PhD, Professor   Member of Committee
Department of Mechanical Engineering

_____

Prof. Mahnoud Al-Hindi, PhD, Associate Professor   Member of Committee
Department of Chemical and Petroleum Engineering

Date of thesis defense: September 13, 2018

AMERICAN UNIVERSITY OF BEIRUT

THESIS, DISSERTATION, PROJECT RELEASE FORM

Student Name:

Seblany	Racha	Youssef

☑ Master's Thesis   ◯ Master's Project   ◯ Doctoral Dissertation

☑ I authorize the American University of Beirut to: (a) reproduce hard or electronic copies of my thesis, dissertation, or project; (b) include such copies in the archives and digital repositories of the University; and (c) make freely available such copies to third parties for research or educational purposes.

☐ I authorize the American University of Beirut, to: (a) reproduce hard or electronic copies of it; (b) include such copies in the archives and digital repositories of the University; and (c) make freely available such copies to third parties for research or educational purposes after:

> **One ---- year from the date of submission of my thesis, dissertation, or project.**
> **Two ---- years from the date of submission of my thesis, dissertation, or project.**
> **Three ---- years from the date of submission of my thesis, dissertation, or project.**

_____   17/9/2018

Signature   Date

ACKNOWLEDGMENTS

AN ABSTRACT OF THE THESIS OF

Racha Youssef Seblany   for   <u>Master of Engineering</u>
                                                    <u>Major</u>: Applied Energy

Title: <u>Humidity Control in a Space Conditioned by a Liquid Desiccant Membrane Chilled Ceiling with Displacement Ventilation</u>

The combined liquid desiccant membrane cooled ceiling (LDMC-C) with displacement ventilation (DV) removes humidity directly from the space. It is an effective method for providing thermal comfort and good air quality since it can operate at lower ceiling temperatures compared to conventional chilled ceiling. However, LDMC-C/DV system does not control humidity in the lower occupied zone which may lead to discomfort and health problems if humidity increases due to changes in occupancy or to high humidity in supply air.

In this work, a method for humidity control is proposed where fraction of the dehumidified cool dry air adjacent to the LDMC ceiling is extracted from the exhaust stream and mixed with the DV supply air stream. The strategy reduces the moisture content of the mixed DV supply air without the need to use any other dehumidification technique in the supply duct. This leads to re-establishing of the thermal comfort conditions in the occupied zone; reducing the cooling requirements of the DV system, and resulting in energy savings. To study the system performance during transient loads, a time-dependent mathematical model of the LDMC-C system was developed and validated experimentally. The validated LDMC-C transient model was then integrated to the mixed DV space model and was applied to a case study to demonstrate its effectiveness in providing acceptable humidity and air quality in the occupied zone and to assess its energy performance. It was shown that during high latent load hours, the relative humidity dropped by an average of 8.72% in the occupied zone within a period of 12 minutes. In addition, when mixing strategy is adopted, energy savings of 24% were achieved compared to conventional dehumidification in the supply duct.

CONTENTS

CHAPTER

NOMENCLATURE

A_c	cross-sectional area of the dehumidifier (m^2)
$A_{c\text{-}BDL}$	cross-sectional area of the boundary layer (m^2)
C	concentration of water per desiccant (kg of H_2O/kg $CaCl_2$)
CC	chilled ceiling
C_p	specific heat (J/kg·K)
COP	Coefficient of performance
DV	displacement ventilation
h_{fg}	latent heat of vaporization of the water (J/kg)
H_m	thickness of the desiccant solution (m)
IAQ	indoor air quality
L_p	length of the dehumidifier panel (m)
$LDMC\text{-}C/DV$	liquid desiccant membrane chilled ceiling with displacement ventilation
$\dot{m}$	mass flow rate (kg/s)
$\dot{m}_{entrained}$	entrained air mass flow rate per unit length (kg/s·m)
q	rate of heat transfer (W)
RH	relative humidity (%)
t	time (sec)
T	temperature (℃)
U_c	overall heat transfer coefficient of the membrane (W/m^2·K)
U_m	overall mass transfer coefficient of the membrane (m/s)
V	velocity of supply air (m/s)
W_{th}	width of the membrane (m)
ω	humidity ratio (kg of H_2O/kg of dry air)
x	horizontal distance from the inlet of the membrane (m)
c	CO_2 concentration in air (ppm)
f	fraction of exhaust air mixed with supply air

Greek Letters

δ	boundary layer thickness (m)
μ	dynamic viscosity (kg/m^2.s)

ρ	density (kg/m^3)

Subscripts

a	room air
BDL	boundary layer
CO$_2$	Carbon dioxide
electric	electric appliances
ex	exhaust
latent	latent heat generated by people
light	lighting equipment
outside	outside air
people	sensible heat generated by people
s	supply air conditions
sol	solution
w	wall

ILUSTRATIONS

TABLES

CHAPTER I

COOLED LIQUID DESICCANT MEMBRANE CEILING WITH MIXED DISPALCEMENT VENTILATION

A. Introduction

Chilled ceilings (CC) have recently attracted attention due to their unique features in providing cooling that results in thermal comfort of occupants at low noise while using less energy compared to conventional cooling systems (Riffat et al., 2004; Miriel et al., 2002; Hao et al., 2007). However, two main concerns are presented in such systems are: the indoor air quality and the limit on the minimum ceiling temperature. The first concern is due to the absence of a ventilation system while the second concern is attributed to the risk of condensation. Therefore, it is preferable to equip the CC system with an additional ventilation system such as the displacement ventilation (DV) (Feustel and Stetiu, 1995). The DV system removes additional sensible and latent load as well as pollutants from the indoor air (Novoselac and Srebric, 2002). So, the latent load removal and humidity control in the CC/DV conditioned space is completely reliant on the DV supply airflow conditions to deliver a comfortable environment with good indoor air quality (Imanari et al., 1999; Zhang and Niu, 2003).

Although the DV system has solved the first drawback of the CC system but the risk of condensation remains if the temperature of ceiling is not simultaneously controlled with the humidity content of the DV supply air (Tang et al., 2016; Mumma, 2003). In order to prevent any risk of condensate formation on the ceiling, researchers have considered the use of liquid desiccant with hydrophobic membranes to dehumidify the air without direct contact with the desiccant (Fauchoux et al., 2009; Hemingson et al., 2011;

Eldeeb et al., 2013; Haung et al., 2014). Recently, liquid-to-air membrane energy exchangers (LAMEEs), capable of achieving significant energy savings when integrated with conventional air-conditioning systems (Abdel-Salam et al., 2014), were developed and tested. The performance of the LAMEE was further enhanced by designing a 3-fluid LAMEE to control the temperature of the desiccant solution, which represented a challenge in conventional 2-fluid LAMEEs (Abdel-Salam et al., 2016; Abdel-Salam et al., 2016; Abdel-Salam et al., 2017). In liquid desiccant-membrane systems, the membranes that are permeable for water vapor but impermeable for liquid desiccant can be installed inside the space to directly pick up the moisture from the vicinity of the membrane (Keniar et al., 2015). In the work of Muslmani et al. (2016) and Hout et al. (2017), the desiccant-membrane system was used as cooled ceiling surface integrated with a displacement ventilation system (LDMC-C/DV). The integrated desiccant membrane cooled ceiling and displacement ventilation system (LDMC-C/DV) resolved the problem of condensation and allowed lower ceiling operating temperatures. Such low ceiling temperature cannot normally be used in conventional CC/DV systems due to the condensation risk. The LDMC-C/DV system succeeded in providing comfortable indoor conditions for a certain range of DV supply air temperature and humidity (Hout et al., 2017). However, the dehumidification in the membrane system occurred at the ceiling level only. Thus, if the system is not equipped with a control strategy for the humidity content of the DV supply air, moisture accumulation can build up in the occupied zone jeopardizing the thermal comfort of the occupants. An indoor relative humidity that exceeds 70% can lead to a sensation that the skin is "wet and sticky" (Dougherty, 2011). Moreover, elevated moisture levels within the occupied zone can induce mold growth, respiratory problems, corrosion and chemical deterioration of the

building materials (Bornehag et al., 2004; Straube, 2002). Therefore, it is of interest to find a strategy that allows the integrated LDMC-C/DV system to control the indoor humidity in order to extend its applicability to cover the extreme outdoor environmental conditions.

Researchers have used various strategies to dehumidify the air outside the space. A typical dehumidification method in DV systems is to cool the supply air to below its dew point temperature to remove the moisture via condensation (Straube, 2002; Bahman et al., 2012). The air is subsequently re-heated to the desired supply temperature to the occupied zone (Abdel-Salam et al., 2013). This method is an energy intensive technique (Qi et al., 2012). Another well-known dehumidification strategy is the use of solid desiccant in the DV supply stream (Mazzei et al., 2005; Kabeel, 2009). However, this technique adds complexity to the system and requires energy. Liquid desiccant systems tower beds have also been considered to efficiently dehumidify the supply air outside the space (Tu et al., 2009; Liu et al., 2018). The liquid desiccant system is often integrated with a sustainable energy source which reduces the system energy demand (Öberg and Goswami, 1998). However the problem with liquid desiccant tower beds is the direct contact between the supply air and the hazardous desiccant that can lead to potential health issues (Studak and Peterson, 1988).

In LDMC-C/DV systems, the dehumidification takes place near the ceiling and has no direct effect on the humidity in the lower zone since the cool dry adjacent to the ceiling is exhausted. To take advantage of this fact, a fraction of the dry and cool exhaust air could be mixed with the DV supply air when outdoor conditions are humid. This simplified technique can result in reducing the humidity in the supply stream which subsequently would lead to a drop in the relative humidity in the occupied zone inside the

space. The main advantage of this technique is basically the reduction in energy consumption and the compactness of the system compared to other dehumidifying techniques (Nielson, 2007; Yuill and Yuill, 2008). Chakroun et al. (2011) used this procedure of mixing exhaust cool air with outdoor supply air in conventional CC/DV and reported energy savings of up to 20.6% compared to the case of the 100% fresh air DV supply. However, this technique is constrained by the maximum allowed CO_2 concentration needed for good IAQ in the occupied zone (Kanaan et al., 2010) which must not exceed the recommended ASHRAE standards (ASHRAE, 2007). Consequently, for non-humid conditions, no mixing is needed between the exhaust and supply air, and the IAQ would be maintained by the DV system, while in extreme humid conditions, a fraction of the dry and cool exhaust air are mixed with the supply air in LDMC-C/DV system.

Therefore, the objective of this work is to propose a humidity control strategy based on mixing the exhaust dry cool air with the supply fresh air in LDMC-C/DV conditioned spaces. A transient model of the integrated LDMC-C/DV system is developed based on Hout et al. steady state model (Hout et al., 2017). The model incorporates the changing supply and exhaust conditions during the implementation of the mixing strategy and is composed of the space model and the membrane boundary layer model. The transient membrane boundary layer model is validated experimentally. The integrated model is applied to a case study of an office space in Beirut during humid summer conditions. The effectiveness of the humidity control strategy in LDMC-C/DV system and the associated energy savings are then evaluated in comparison with the conventional sub-cool reheat humidity control strategy at identical supply conditions.

4

B.   System description

In this work, it is proposed to integrate the LDMC-C/DV system with a humidity control strategy. The main advantage of such integrated system is basically the potential energy savings compared to conventional cooling system while providing the thermal comfort in the space, lower noise, and good indoor air quality. The main constraints in the system are the maximum allowable concentration of CO_2 to maintain acceptable IAQ and the allowable relative humidity for maintaining thermal comfort in the occupied zone. If the relative humidity increases dramatically in the supply air, a larger fraction of the exhaust air must be mixed with fresh air leading to higher CO_2 concentration. Thus, this mixing strategy must control the inlet humidity, while affording an acceptable concentration level of CO_2.

Fig. 1a shows a schematic of the integrated LDMC-C/DV system with the proposed mixing strategy of humidity control in which a fraction of exhaust air is mixed with incoming fresh air. The LDMC-C/DV system is composed of the desiccant membrane ceiling and the displacement ventilation system. The desiccant solution, which is flowing over the ceiling membrane, removes the heat and moisture from the air at the vicinity of the membrane. The DV system supplies fresh air into the space at the floor level. The supplied air warms up due to the heat generated by the occupants and the appliances and moves upward to the ceiling level due to buoyancy effect (Cho et al., 2005). This creates two large zones; the lower occupied zone which contains fresh cool air and the upper recirculation zone which contains the warm contaminated displaced air. The two zones are separated by the stratification height defined as the height at which the flow from the thermal plumes originating from internal load elements becomes equal to the supply flow rate (Kanaan et al., 2010). Air is exhausted near the ceiling membrane where it is partly

drawn from the boundary layer formed near the cooled membrane ceiling and from the upper recirculation zone. The near ceiling air boundary layer exchanges heat and mass with the liquid desiccant solution and the air flowing in that zone is relatively cool and dry.

In this work, the LDMC-C/DV system is modified by implementing a control strategy of the humidity in the occupied zone. The proposed strategy is based on mixing a fraction of the exhausted air, which has lower temperature and humidity than outdoor conditions, with the supply air stream as demonstrated in the process laid on the psychrometric chart shown in Fig. 1b. On the air side, a fraction of the exhaust air (f) is mixed with the outside fresh air (a) that has been subjected to sensible cooling with the remaining fraction of the exhaust air (b). The mixed air (c) is introduced into a cooling coil to sensibly cool it down to a pre-defined set point supply temperature (d) without any effect on its humidity ratio. The mixed air supply leaving the coil is introduced into the space near the floor level where it displaces the warmer air to the upper zone (e) and to the near ceiling boundary layer to exchange heat and water vapor with the desiccant solution and the cycle is repeated. The desiccant solution cycle starts by the flow of the desiccant solution that enters the ceiling panel to remove the heat and moisture from the air at the vicinity of the membrane. Afterwards, the desiccant solution leaves the membrane ceiling panel and enters the regeneration cycle where it is heated to remove the absorbed moisture. Before re-entering the space, the desiccant is cooled by chilled water through a heat exchanger.
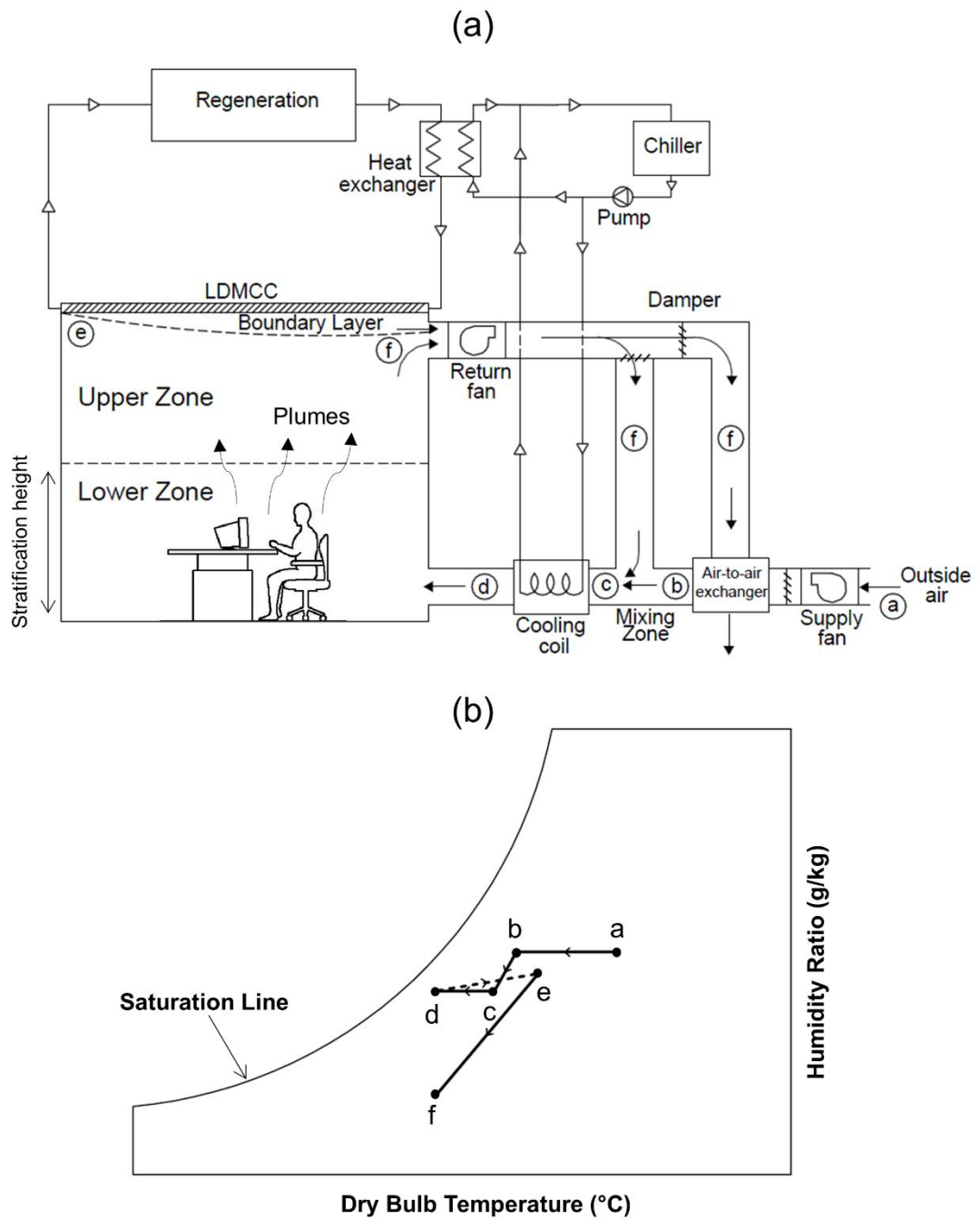
Figure 1: Schematic of the (a) LDMC-C/DV system with mixed supply; (b) system operation cycle on psychrometric chart

CHAPTER II

DEVELOPMENT OF TRANSIENT BOUNDARY LAYER MODEL & INTEGRATION WITH DV SPACE MODEL

The research methodology is based on the integration of two models: the membrane boundary layer model and the cooled-ceiling DV space model. As mentioned in the system description, there is a mass and heat exchange through the ceiling membrane with the air in the ceiling-adjacent boundary layer which entrains air from the space upper zone. The coupled cooled-ceiling model and DV space model predicts the temperature and humidity of the upper zone which are used as input to the membrane ceiling-adjacent boundary layer model. The changes in the air supply conditions affect directly the conditions of the air in the upper zone which is dehumidified in the ceiling-adjacent boundary layer and is subsequently mixed with the supply DV air. The effectiveness of the DV air mixing strategy for humidity control depends on the humidity conditions of the exhausted air near the ceiling. However, the dehumidification in the membrane system is not instantaneous and greatly depends on the ceiling desiccant flow rate. Hence, a transient model for the ceiling membrane system is needed to account for the needed time for the LDMC-C/DV cycle to stabilize.

Therefore, the research methodology starts by deriving a transient mathematical model of the heat and mass transfer through permeable membrane between the solution desiccant and the adjacent air layer where the exhaust grill draws the air forming the near-ceiling boundary layer (Hout et al., 2017). The transient membrane boundary layer model is then integrated with the transient space model developed by Ghali et al. (2007). This is followed by performing experiments to validate the transient model of the heat and mass

transfer through permeable membrane between the desiccant solution and the adjacent air layer.

The effectiveness of the proposed humidity control strategy is then investigated using the integrated model for a case study of an office space located in Beirut, Lebanon and conditioned by a LDMC-C/DV system. In the case study, a fraction of the exhaust air is mixed with the fresh outdoor air for DV supply. The effect of this mixing process on the relative humidity, the thermal comfort and the IAQ within the occupied zone are investigated. Moreover, the energy savings resulting from the proposed humidity control strategy are compared to conventional dehumidification technique of sub-cool and reheat outside the space.

A. Transient mathematical model of the membrane boundary layer (air layer and liquid desiccant flow sides

In order to predict the temperature and the moisture content of the desiccant solution and the air flowing adjacent to the ceiling, transient mass and energy conservation equations are derived and solved in the dehumidification zone (on both air and desiccant sides). The mass and heat transfer balances are applied on both the liquid desiccant side and the air boundary layer side (Hout et al., 2017). The two sides are separated by a membrane which is permeable to water vapor but impermeable to liquid desiccant solution. The heat and mass flows within the boundary layer are shown in Fig. 2. The following assumptions were adopted in the derivation of the model:

(i)   The flow is assumed one dimensional,

(ii)   The latent heat is considered constant due to small temperature gradient (Keniar et al., 2015),

(iii)   The vapor diffusion and the heat conduction in air are assumed negligible,

(iv)   The conditions of the air are assumed lumped in the upper and lower zones of the space (Hout et al., 2017),

(v)   The thicknesses of all boundary layers (velocity, temperature and mass) are considered equal for simplification purposes (Schlichting and Gersten, 2000).

The mass and the heat transfer equations on the desiccant side are given respectively as follows:

$$\underbrace{\rho_{sol}A_c\frac{\partial(C_{sol})}{\partial t}}_{Transient\ term} = \underbrace{-\dot{m}_{sol}\frac{\partial(C_{sol})}{\partial x}}_{Net\ convecttive\ moisture\ flow} + \underbrace{U_mW_{th}\rho_a(\omega_{BDL}-\omega_{sol})}_{Moisture\ transport} \tag{1}$$

$$\underbrace{A_c\frac{\partial(C_{p-sol}T_{sol})}{\partial t}}_{Transient\ term} = \underbrace{-\dot{m}_{sol}\frac{\partial(C_{p-sol}T_{sol})}{\partial x}}_{Net\ convective\ energy\ flow} + \underbrace{U_cW_{th}(T_{BDL}-T_{sol})}_{Sensible\ enrgy\ added}$$

$$+ \underbrace{U_mW_{th}\rho_ah_{fg}(\omega_{BDL}-\omega_{sol})}_{Latent\ energy\ added} \tag{2}$$

where $\dot{m}_{sol}$(kg/s), T_{sol} (K), C_{sol} (kg of H_2O/kg $CaCl_2$), C_{p-sol} (J/kg·K), ρ_{sol} (kg/m^3), ω_{sol} (kg of H_2O/kg of dry air) are the respective solution mass flow rate, temperature, concentration, solution specific heat, density and the humidity ratio; T_{BDL} (K) and ω_{BDL} (kg of H_2O/kg of dry air) are respectively temperature and humidity ratio of the boundary air layer, and h_{fg} (J/kg) is the heat of vaporization of water. U_c (W/m^2·K) and U_m (m/s) are respectively the overall heat and mass transfer coefficient and A_c (m^2) is the cross sectional area of the dehumidifier.

On the other side of the dehumidifier, air is flowing in opposite direction (counter-flow mode). The flow of air near the ceiling is caused by the exhaust grill that draws the

air and forms a near-wall boundary layer. In the following, the transient mass and heat transfer equations are solved in this boundary layer as following:

$$\underbrace{\rho_a A_{c,BDL} \frac{\partial \omega_{BDL}}{\partial t}}_{Transient\ term} = \underbrace{-\dot{m}_{BDL} \frac{\partial(\omega_{BDL})}{\partial x}}_{Net\ convective\ moisture\ flow} + \underbrace{U_m W_{th} \rho_a (\omega_{sol} - \omega_{BDL})}_{Moisture\ transport}$$

$$+ \underbrace{\dot{m}_{entrained} \omega_a}_{\substack{Convective\ moisture\ flow \\ of\ the\ entrained\ air}} \tag{3}$$

$$\underbrace{\rho_a A_{c,BDL} C_{p,a} \frac{\partial T_{BDL}}{\partial t}}_{Transient\ term} = \underbrace{-\dot{m}_{BDL} C_{p,a} \frac{\partial(T_{BDL})}{\partial x}}_{Net\ convective\ energy\ flow} + \underbrace{U_c W_{th} (T_{sol} - T_{BDL})}_{Sensible\ enrgy\ removed} +$$

$$\underbrace{U_m W_{th} \rho_a h_{fg} (\omega_{sol} - \omega_{BDL})}_{Latent\ energy\ removed} + \underbrace{\dot{m}_{entrained} C_p T_a}_{\substack{Convective\ energy\ flow \\ of\ the\ entrained\ air}} \tag{4}$$

where T_a (K) and ω_a (kg of H_2O/kg of dry air) are respectively the temperature and humidity ratio of room air; $\dot{m}_{BDL}$ (kg/s) is the air mass flow rate through the boundary layer across a cross-sectional area of $A_{C,BDL}$ (m^2), and $\dot{m}_{entrained}$ (kg/s·m) is the entrained mass flow rate of air per unit length in the boundary layer and is dependent on x. It was determined by applying the mass balance on a differential element in the boundary layer zone as done previously by Hout et al. (2017).

Desiccant leaving the ceiling

LDMC-C

Desiccant entering the ceiling

Boundary layer

Air flow

(b)

$\dot{m}_{sol}, T_{sol}, C_{sol}$

Desiccant Outlet

Desiccant Inlet

$\dot{m}_{BDL}, T_{BDL}, W_{BDL}$

$m_{entrained}$

$\updownarrow$: heat and mass exchange through the porous membrane

$\nearrow$: entrainment from the upper zone
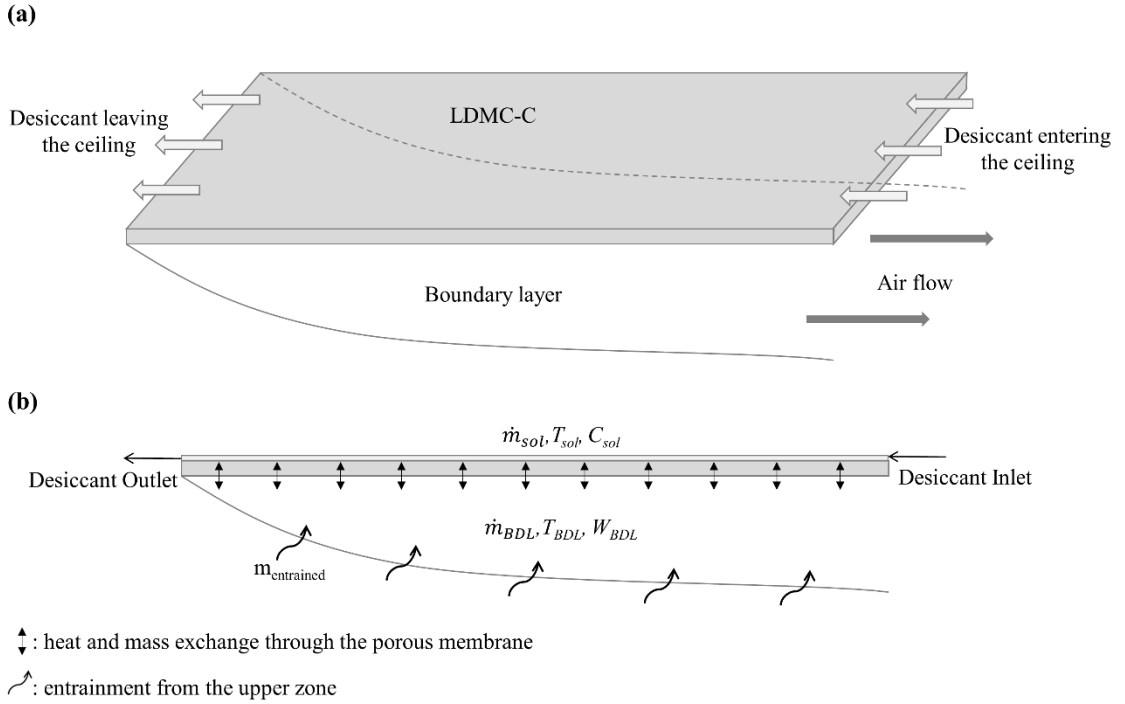
Figure 2: (a) Schemetic of the LDMC-C with the attached boundary layer; (b) Cross-sectional area of the boundary layer with the heat and mass exhange shown inside

B. Integration with the DV space model

The temperature and humidity ratio of the air in the boundary layer are directly related to the conditions inside the space. Therefore, the prediction of the air temperature and moisture content in the near-wall boundary layer necessitates the integration of the model with a transient DV space model in presence of a cooled ceiling (Ghali et al., 2009). The space model predicts the conditions of air in the upper and lower zones that are separated by the stratification height. The correlations used to calculate the stratification height are detailed in the previous work (Hout et al., 2017) and will not be repeated here. In this study, the integrated model is modified in order to incorporate the effect of mixing a portion of the exhaust air with the supply air of the space model. Therefore, the moisture

content of the supply air ωs depends on the moisture content of both the exhaust air (ω_{ex})

and the outside fresh air ($\omega_{outside}$) as well as the mixing fraction (*f*) as follows:

$$\omega_s(t) = f \cdot \omega_{ex}(t) + (1 - f) \cdot \omega_{outside} \tag{5}$$

The exhaust air is a mixture of the air leaving the boundary layer and some air exhausted

from the upper zone as shown in Fig. 3, and has a flow rate equal to that of the DV supply.

The lumped air conditions (temperature and humidity ratio) inside the space are

predicted from the mass and energy balance equations in the upper unoccupied zone and

the lower occupied zone as follows:

1. *Upper unoccupied space model zone:*

$$\underbrace{m_a \frac{\partial \omega_a}{\partial t}}_{\substack{transient\ term}} = \underbrace{\dot{m}_S \omega_{a,o}}_{\substack{convective\ moisture \\ exchange}} - \underbrace{\int_0^{L_p} \dot{m}_{entrained}(x)\omega_a dx}_{\substack{Convective\ moisture\ flow \\ of\ the\ entrained\ air}} -$$

$$\underbrace{\dot{m}_{ex}\omega_a}_{\substack{moisture\ flow\ through \\ the\ exhaust}} \tag{6}$$

$$\underbrace{m_a C_{p,a} \frac{\partial T_a}{\partial t}}_{\substack{transient\ term}} = \underbrace{\dot{m}_S C_{p,a} T_{a,o}}_{\substack{convective\ heat \\ exchnage}} - \underbrace{\int_0^{L_p} \dot{m}_{entrained}(x)C_{p,a}T_a dx}_{\substack{Convective\ energy\ flow \\ of\ the\ entrained\ air}} - \underbrace{\dot{m}_{ex}C_{p,a}T_a}_{\substack{energy\ flow\ through \\ the\ exhaust}} +$$

$$\underbrace{q_{light}}_{\substack{lighting\ load}} + \underbrace{\sum(h_i A_{w,i}(T_{W,i} - T_a))}_{\substack{convective\ heat\ exchange\ with \\ the\ walls}} \tag{7}$$

2. Lower occupied space model zone:

$$\underbrace{m_{a,o}\frac{\partial \omega_{a,o}}{\partial t}}_{transient\ term} = \underbrace{\dot{m}_S\left(\omega_S(t) - \omega_{a,o}\right)}_{\substack{net\ convective \\ moisture\ transfer}} + \underbrace{\frac{q_{latent}}{h_{fg}}}_{\substack{occupants\ latent \\ load}} \qquad (8)$$

$$\underbrace{m_{a,o}C_{p,a}\frac{\partial T_{a,o}}{\partial t}}_{transient\ term} = \underbrace{\dot{m}_S C_{p,a}\left(T_S - T_{a,o}\right)}_{\substack{net\ convective\ heat \\ transfer}} + \underbrace{\sum\left(h_i A_{w,i}\left(T_{W,i} - T_{a,o}\right)\right)}_{\substack{convective\ heat\ exchange\ with \\ the\ walls}} + \underbrace{q_{electric}}_{electric\ load} +$$

$$\underbrace{q_{people}}_{\substack{occupants\ sensible \\ load}} \qquad (9)$$

where $T_{a,o}$ (K) and $\omega_{a,o}$ (kg of H_2O/kg of dry air) are the respective temperature and humidity ratio of air in the occupied zone. m_a and $m_{a,o}$ (kg) are the mass of air in the upper and lower zones respectively. T_s (K), ω_s (kg of H_2O/kg of dry air) and $\dot{m}_S$ (kg/s) are the respective temperature, humidity ratio and mass flow rate of the supply air. $\dot{m}_{ex}$ (kg/s) is the mass flow rate of the exhaust air, and L_p (m) is the length of the dehumidifier panel.
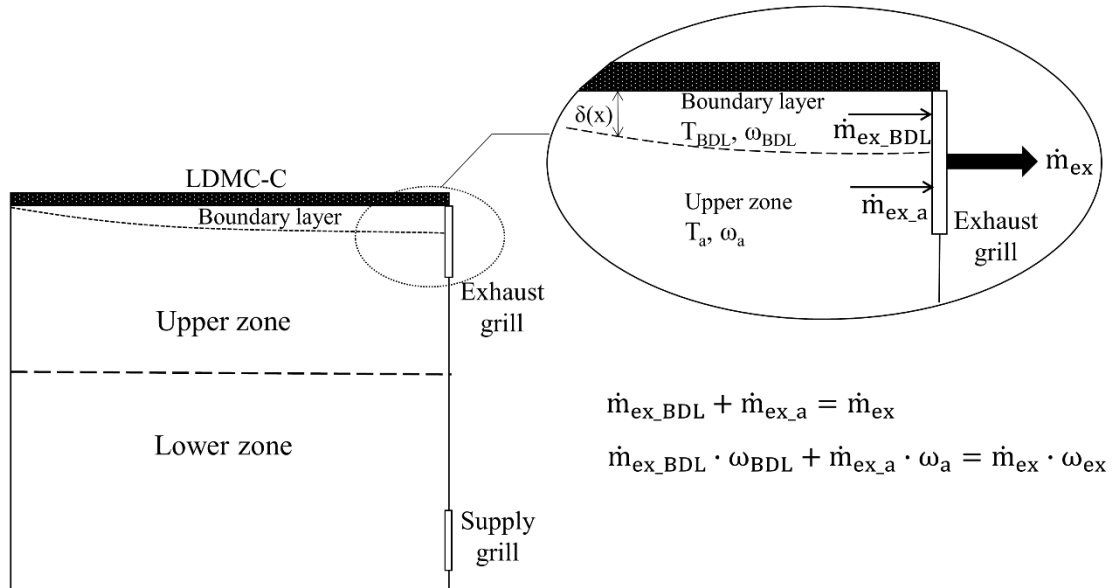
Figure 3: Mass balance of air at the exhaust of the LDMC-C/DV system

C. Numerical Methodology of the integrated LDMC-C/DV model with the exhaust air/supply air mixing strategy

The integration of the membrane boundary layer model and the space model is mainly related to the fact that the conditions of air in the boundary layer are dependent on the conditions of the air in the unoccupied upper zone. Moreover, the use of the mixing strategy for humidity control in the lower zone enforces the coupling between the two models. Fig. 4 illustrates the flow chart of the current integrated LDMC-C/DV model. The conditions were initialized at t = 0 and an implicit scheme is used with a time step of 0.5 s. The implicit method was used because of its stability even when large time steps were used. At each time step, the temperature and the humidity ratio of the unoccupied zone (T_a, ω_a) were assumed. The membrane boundary layer model was simulated at the current time step, and the exhaust humidity ratio (ω_{ex}) was predicted and used as an input to find the supply air conditions of the space model. At the same time step, the space model was simulated in order to predict the new values of the temperature and the humidity ratio of the upper zone (T_a, ω_a) to be updated in the membrane boundary layer model. These steps were repeated until the absolute relative error between the current and previous iteration of the temperature and the humidity ratio of the unoccupied zone (T_a, ω_a) is minimal. After reaching the convergence at the current time step, the integrated model advanced in time and solved for the output parameters of the next time step until the desired simulation time is attained.

Each of the two models has its own input and output parameters. The input parameters of the membrane boundary layer model are basically the geometrical dimensions of the system, the physical properties of the membrane, the conditions of the air coming from the unoccupied zone (T_a, ω_a) and the inlet conditions of the solution desiccant

15

(temperature, concentration and mass flow rate). The output parameters of this model are the instantaneous conditions of air side and solution desiccant side. The model was based on solving the set of mass and heat transfer equations on both the liquid desiccant side and the air boundary layer. Therefore, equations (1-4) were discretized in the axial direction using a finite volume approach. At each time step simulation, iterations were performed to correct the air and desiccant conditions. Once convergence was reached, the exhaust air condition was used to find the supply air condition to the space model using equation (5). For given space geometry, the space model input parameters are the DV supply flow rate and temperature. Other input parameters included the outdoor environmental conditions and the thermal and latent loads in the space. The cooled-ceiling DV space model was used to solve the mass and heat equations taking into account the thermal plumes from the internal heat sources as well as wall plumes and radiative exchange with the ceiling. The model predicted the temperature and humidity ratio of air in the unoccupied zone which represented an input for the boundary layer model. In addition, the DV space model predicted the air conditions (temperature and humidity) within the lower occupied zone which were essential to determine the level of occupants' thermal comfort. The temperature of the walls and ceiling were first assumed and updated iteratively until convergence was achieved when relative error in the air temperature and humidity is less than 10^{-6}.
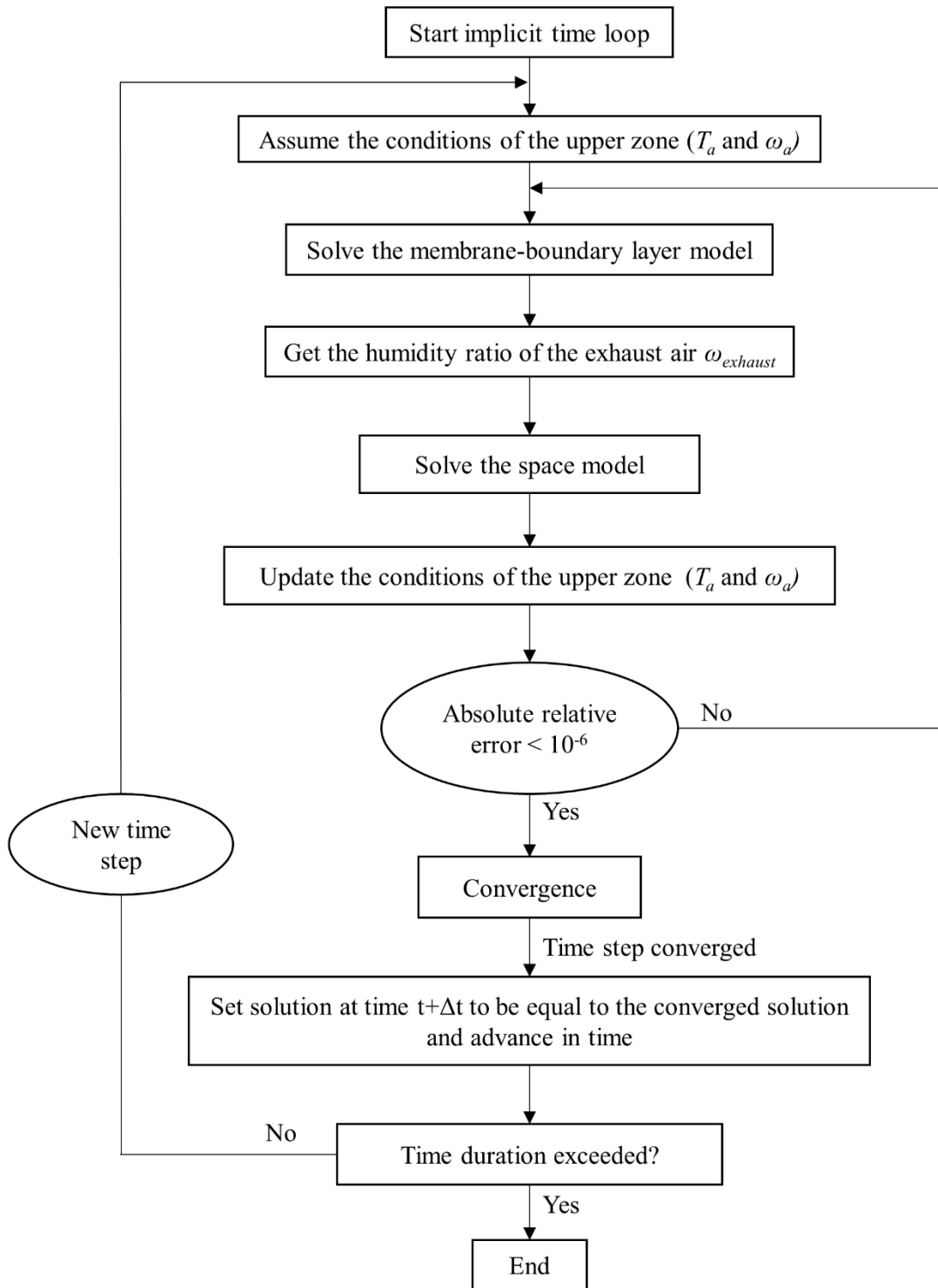
Figure 4: Flowchart of the integrated model

CHAPTER III

EXPERIMENTAL SETUP & MODEL VALIDATION

The objective of the experiment is to validate the membrane boundary layer model and ensure its robustness in predicting the transient behavior of the desiccant solution flow and air boundary layer conditions when a sudden change in humidity content occurs at the supply conditions. This was achieved by conducting an experiment and comparing the model predictions with measured (i) instantaneous moisture removal by the desiccant solution; (ii) instantaneous temperature distribution in the desiccant; (iii) instantaneous temperature distribution air flow when sudden change in the supply relative humidity occurs.

A. Experimental Setup

Since the objective of this experiment is to capture the transient changes of air relative humidity, air temperature, solution temperature and concentration, it is important to use sensors of relatively small response time. For the temperature measurements, PLTC-type thermocouples (OMEGA series, 0.01 ℃ accuracy) of 10 seconds response time were used for both the desiccant solution and the flowing air. The relative humidity of air was measured using relative humidity sensors (OMEGA HX94A series, 2.5% accuracy) of 10 seconds response time. Finally, the solution desiccant concentration was measured by Anton Paar density meter (DMA4500M) with a measuring time of 30 seconds per measure.

Fig. 5-a illustrates the experimental set up in which an open liquid desiccant membrane cycle is used. The experiment was basically composed of a climatic chamber of 1m × 1m × 1m dimensions equipped with supply and exhaust grills of 25cm × 25cm and 50cm × 15cm dimensions respectively. The supply grill was situated at the floor where Honeywell BH-860E humidifiers of 0.4 *l/hr* supply flow rate are placed. The exhaust grill was located at the chamber ceiling level and was connected to an axial fan to draw the air. A rectangular Plexiglas frame of 87 cm length, 20 cm width and 1 cm height is composed of five Propylene membrane sheets bought from Sterlitech (Kent, WA, USA) and were placed at the ceiling level of the chamber room. The membrane has thickness of 0.2 µm, porosity of 80%, and thermal conductivity of 0.0608 W/m·K (Hout et al., 2017). The membrane panel assembly is shown in Fig. 5-b. Baffles were installed along the panel in order to direct the flow of the desiccant and assure that it covers the whole panel. Moreover, the baffles reinforce the membranes, and help in reducing deflection and avoiding mal-distribution of the flow. The desiccant solution used in the experiment was Calcium Chloride ($CaCl_2$). The desiccant solution was stored in a plastic reservoir situated outside the chamber. A small pump with a globe valve was installed to deliver the desiccant solution from the storage container to a cooling bath where the desiccant temperature was brought down and passed into the ceiling membrane panel system. In order to track the changes of the desiccant solution conditions, the thermocouples and the density meter were immersed in the desiccant solution. Meanwhile, the conditions of the air were measured by the thermocouples and the relative humidity sensors located near the start and the exhaust in the air side very close to the membrane panel.

(a)

(b)
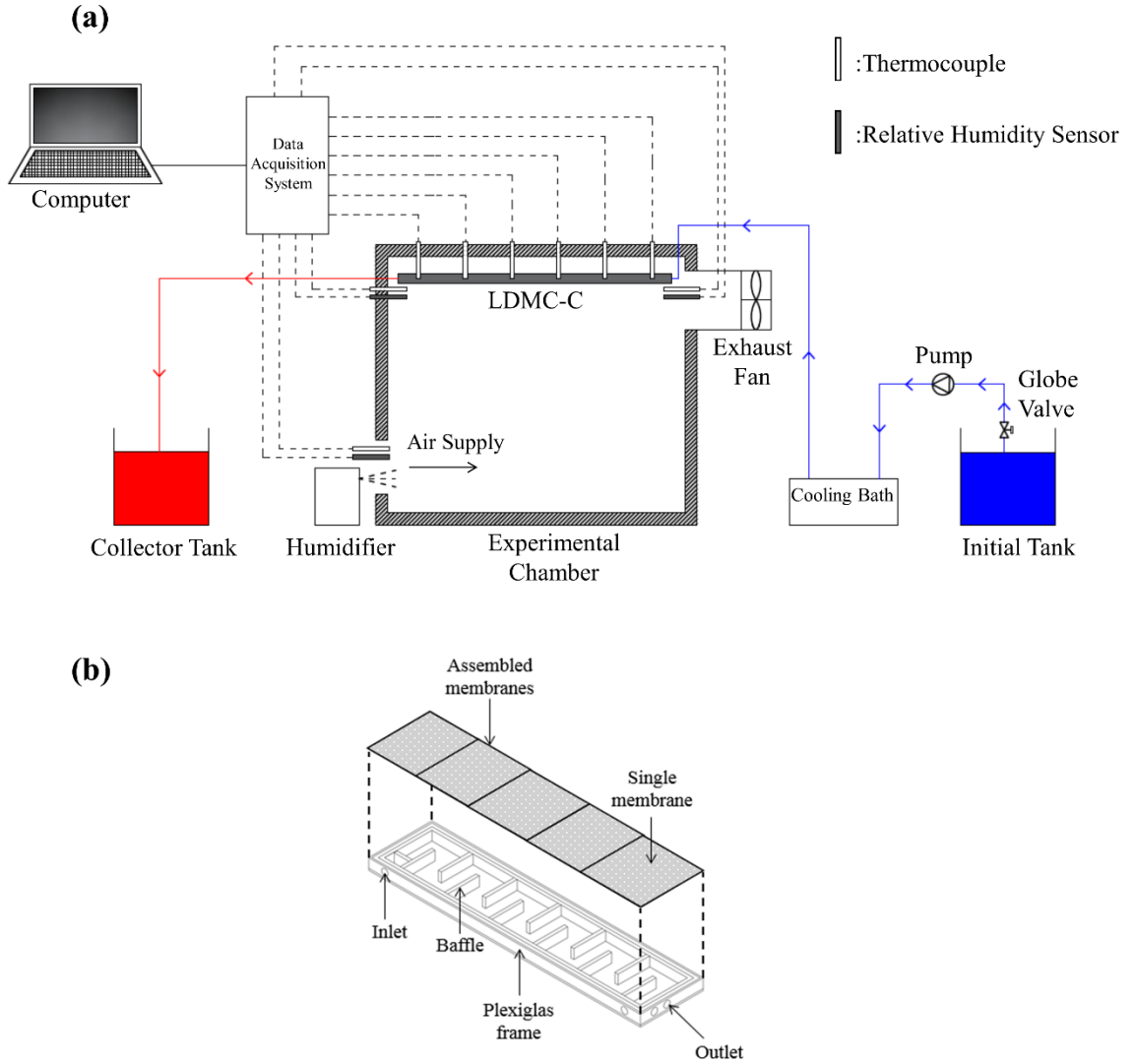
Figure 5: (a) Schemtic of the experimental setup; (b) Schemtic of the membrane-panel assembly

B. Experimental Protocol

The experiment was conducted in two phases. In the first phase, a humidifier was used at the supply grill, and the experiment was run until steady state conditions were achieved. In the second phase, the supply air conditions (temperature and humidity) were changed abruptly so that the transient change can be observed in the temperature and the relative humidity measured at both air and desiccant sides. In both phases, the ambient temperature and relative humidity surrounding the chamber were measured to be 23 ± 0.8

°C and 57 ±3% respectively. The two phases of the experiments are summarized as follows:

Phase 1: The first phase started by turning on the pump and regulating the flow to the desired value (8.4 *ml/s*) using the globe valve and a flow meter (STVSV) of ± 0.1 *ml/s* accuracy. Meanwhile, the exhaust fan and the humidifier were turned on. The desiccant solution was pumped from its reservoir to the cooling bath where it was cooled down to 12°C (± 0.5°C). The desiccant solution enters the panel; in the meantime, the air was supplied in the opposite direction after being humidified by the humidifier located close to the supply grill. In this phase, the supply temperature was 20.14°C (± 0.5°C) and the relative humidity was 66.9% (± 2.5%). The steady state conditions were reached and no significant change was observed in the measurements of temperatures and humidity of the near-ceiling air and the desiccant solution.

Phase 2: In the second phase, a sudden increase in the moisture content of the supply air that was increased by 22% from 0.0098 to 0.0112 (*kg of H$_2$O/kg of dry air*). This increase in the supply moisture content was accompanied by a slight drop in the supply air temperature. The supply air temperature and humidity at the supply became 19.2°C (± 0.5°C) and 80.22% (± 2.5%) respectively.

The two-phase experiment was repeated three times to ensure repeatability and accuracy of the measurements.
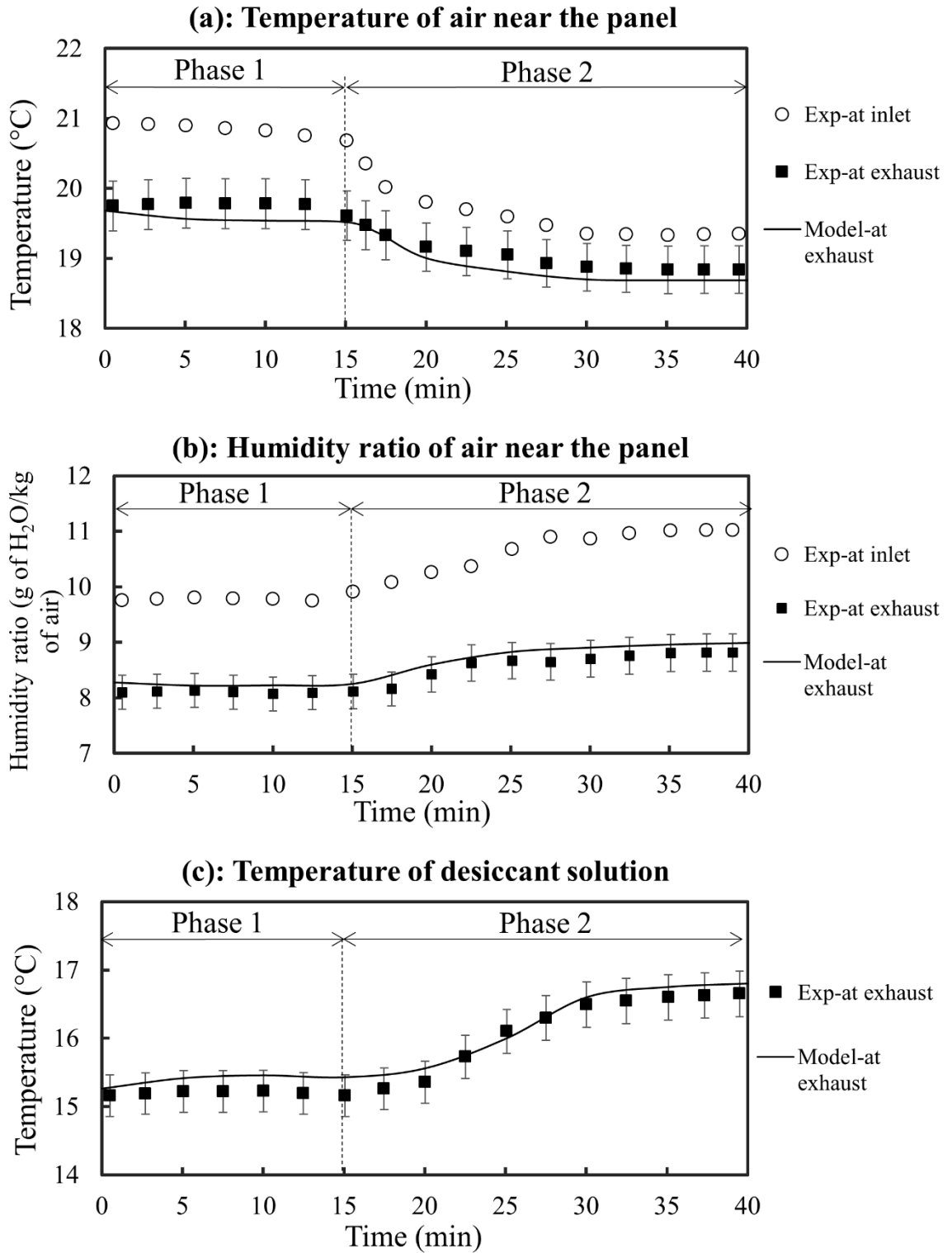
C. Experimental validation

In this section, the predictions of the membrane boundary layer model are compared to the experimental measurements. Simulations were performed based on the actual parameters of the experimental setup, and the measured inlet conditions of the desiccant

solution and the supply air. Fig. 6 shows the experimental measurements and model predictions of (a) temperature and (b) humidity ratio respectively of air near the start and end position of the membrane panel, in addition to (c) the desiccant solution temperature at the exhaust of the panel. The humidity ratio was calculated using the measured temperature and relative humidity of air.

In phase 1, the air was supplied at a temperature and humidity of 20.14ºC (± 0.5°C) and 9.8 (± 0.4) g of H_2O/kg of dry air respectively, and the desiccant solution was introduced at 12 ºC with a flow rate of 8.4 ml/s. Moreover, the inlet desiccant solution concentration was measured to be 37.48 ± 0.01% (1.6681 kg of H_2O/kg $CaCl_2$). Fig. 6-a and **6-b** show that the measured temperature of the air near the inlet of the membrane panel was close to the supply air temperature (20.9 ºC ± 0.4) and the measured humidity ratio was identical to the supply humidity ratio (9.8 ±0.3 g of H_2O/kg of dry air) since there was no internal moisture generation. The air temperature and humidity ratio near the outlet of the panel were lower by 1ºC and 1.8 g of H_2O/kg of dry air respectively, because of the heat and mass exchange with the desiccant throughout the panel length. Fig. 6-c shows that the temperature of the desiccant leaving the panel increased to around 15.2 ºC (± 0.3°C) due to the latent and sensible heat added from the air near the panel surface through the permeable membrane.

In phase 2, the air supply conditions were changed to 19.2ºC and 11.2 g of H_2O/kg of dry air. Consequently, a transient variation in the near-ceiling air properties (temperature and humidity) and in the desiccant temperature was observed. It can be seen in Fig. 6-a and 6-b that the temperature of air at the inlet of the membrane panel dropped following the decrease in the supply temperature and reached a steady value of 19.6ºC (± 0.4°C); whereas the humidity ratio underwent a jump induced by the increase in the

moisture generation of the humidifier (from 9.8 to 11.2 g of H_2O/kg of dry air). Accordingly, the air temperature and humidity at the outlet of the membrane panel reached new steady values of 18.6ºC ($\pm$ 0.4°C) and 8.9 ($\pm$ 0.3) g of H_2O/kg of dry air. Furthermore, Fig. 6-c shows that the temperature of the solution experienced a further increase from 15.2 to 16.8 °C ($\pm$ 0.3°C). This is due to the resulting transient change in the properties of air in the vicinity of the panel. The time taken to reach the steady state was about 13 minutes. Good agreement was found between the model predictions and the experimental measurements of temperature and humidity with respective relative errors of 5% and 7.3%. As for the desiccant solution temperature, the maximum relative error between the measured and predicted values was no more than 4.8%. Furthermore, concentration measurements showed that the desiccant concentration has increased in phase 2 to 1.6687 (kg of H_2O/kg $CaCl_2$). The predicted concentration of the leaving desiccant was rather accurate (0.01% percentage error) and found to be 1.6685 (kg of H_2O/kg $CaCl_2$).

(a): Temperature of air near the panel

(b): Humidity ratio of air near the panel

(c): Temperature of desiccant solution

Figure 6: Variation with time of the experimental and predicted values of: (a) the temperature of air near the ceiling, (b) the humidity ratio of air near the ceiling and (c) the temperature of desiccant leaving the panel

CHAPTER IV

APPLICABILITY OF THE HUMDIITYCONTROL STARTEGY TO A CASE STUDY IN BEIRUT

A. Description of the case study

In order to investigate the effect of the proposed control strategy on reducing occupied zone humidity with LDMC-C/DV system, a test case is applied to a typical office space located in Beirut city and conditioned by LDMC-C/DV system. The office has dimensions of 5 m × 5m × 3m, and is characterized by internal loads. The office space is occupied from 7:00 am to 7:00 pm with a maximum occupancy of 6 persons. The dynamic latent and sensible loads are based on the occupancy schedule and are shown in Table 1, while the load from equipment and lights is fixed at 500 W. The peak load due to internal loads is around 82 W/m^2. The case study is demonstrated for a typical summer day of Beirut (August 15th) and the ambient conditions at which the case study is simulated are shown in Table 1.

The used liquid desiccant in the chilled ceiling membrane is Calcium Chloride (CaCl$_2$) of a mass concentration of 38% to avoid the risk of crystallization. The conditions at the desiccant-membrane ceiling are fixed by introducing the desiccant solution at constant temperature (13ºC) and flow rate (0.5 kg/s). At the level of the DV system, the supply air is cooled, without any dehumidification, to a constant pre-defined temperature of 20ºC. In order to handle the dynamic internal load, the DV supply flow rate is varied to maintain the stratification height between 1.1m and 1.5m.

Table 1: Internal loads and ambient conditions in the occupied zone in an office space in Beirut, Lebanon

Time	Internal sensible load (W)	Internal latent load (W)	Ambient temperature (ºC)	Ambient humidity ratio (g of H_2O/kg of air)
7:00-8:00	1000	75	24.50	13.15
8:00-9:00	1550	95	25.80	13.15
9:00-10:00	1650	150	27.30	13.93
10:00-11:00	1650	150	28.70	14.81
11:00-12:00	1650	150	29.90	15.52
12:00-13:00	1700	300	30.70	16.28
13:00-14:00	1700	350	31.30	16.67
14:00-15:00	1700	350	31.60	16.87
15:00-16:00	1150	200	31.60	16.71
16:00-17:00	1050	150	31.10	16.44
17:00-18:00	950	100	30.10	15.75
18:00-19:00	1050	150	29.10	15.09

1. *Base case without humidity control:*

The simulation of the typical office was achieved for the base conventional case. The integrated LDMC-C/DV model simulations were based on the internal loads and ambient conditions of space occupied zone (see Table 1). In addition, the DV supply flow rate used in the simulation was varied within the range of 0.08-0.26 kg/s to maintain the stratification height above 1.1 m (Keblawi et al., 2009). The results of the simulation are summarized in Table 2. It was found that the air temperature within the occupied zone varied between 23.78ºC and 25.55ºC while the relative humidity ranged between 54.44% and 78.77%. The peak humidity was between 14:00 and 15:00 hr due to the combined effect of the latent load (350 *W*), and the outside humid air (16.872 *g* of H_2O/kg of dry air). Between 12:00-15:00 hr, the relative humidity exceeded 70% while the space

temperature was about 25.5 °C. This relatively high humidity will cause mold growth, respiratory problems, and human discomfort. The latter effect is shown by the predicted mean vote (PMV) value that exceeded 0.5 (0.52 and 0.53). Therefore, a humidity control strategy based on mixing a fraction of the exhaust air with the fresh DV supply was implemented between 12:00 till 15:00 hr to verify its ability in reducing the relative humidity inside the space and re-establish thermal comfort conditions.

Table 2: Hourly results of the base case without humidity control

Time	Supply air flow rate (kg/s)	Air temperature in the occupied zone (ºC)	Relative humidity in the occupied zone (%)	Air temperature in the upper zone (ºC)	PMV	Stratification height (m)
7:00-8:00	0.082	24.31	54.44	24.37	0.21	1.10
8:00-9:00	0.166	25.32	60.04	24.77	0.35	1.40
9:00-10:00	0.177	25.53	63.84	24.82	0.42	1.42
10:00-11:00	0.177	25.52	67.77	24.68	0.46	1.42
11:00-12:00	0.177	25.51	71	24.57	0.49	1.42
12:00-13:00	0.185	25.54	75.07	24.47	0.52	1.47
13:00-14:00	0.184	25.55	77.21	24.41	0.53	1.47
14:00-15:00	0.185	25.53	78.77	24.34	0.53	1.47
15:00-16:00	0.089	25.06	70	24.18	0.47	1.11
16:00-17:00	0.081	24.57	68.10	23.98	0.34	1.10
17:00-18:00	0.08	24	67.19	23.55	0.19	1.10
18:00-19:00	0.08	24.67	62.41	24.28	0.32	1.10

2. *Case study with humidity control implementation:*

The high relative humidity (above 70%) between 12:00 and 15:00 hr could be reduced if a proper humidity-control strategy is applied at the level of the DV supply. This can be achieved by incorporating a mixing system that takes advantage of the cool and dry exhaust air (Fig. 1). For this purpose, a portion of the exhaust air was mixed with the supply air stream while maintaining an appropriate level of IAQ. Thus, the mixing proportion *f* is constrained by the maximum allowed indoor carbon dioxide concentration to maintain acceptable IAQ. For this reason, this proportion *f* must satisfy the following mass conservation equation of carbon dioxide, such that the exhaust air CO_2 concentration is less than 700 ppm (ASTM, n.d.):

$$\frac{\dot{m}_{supply}}{\rho_a} \cdot \left[\underbrace{(1-f) \times c_{fresh}(t)}_{\substack{concentration\ of\ CO_2 \\ in\ th\ portion\ of\ fresh\ air}} + \underbrace{f \times c_{ex}(t-1)}_{\substack{concentration\ of\ CO_2 \\ in\ the\ portion\ of\ exhaust\ air}} \right] + \underbrace{\dot{V}_{generated}(t) \times \rho_{CO_2}}_{CO_2\ generation\ rate} =$$

$$\frac{\dot{m}_{ex}}{\rho_a} \times \underbrace{c_{ex}(t)}_{\substack{concentration\ of\ CO_2 \\ in\ exhaust\ air}} \qquad\qquad (10)$$

where $\dot{V}_{generated}(t)$ is the flow rate of the CO_2 generated by the occupants at the current time and is taken according to the CO_2 generation schedule of Keblawi et al. 9Keblawi et al., 2011), $c_{fresh}(t)$ is the CO_2 concentration in the fresh air at the current time and is taken as 450 ppm. $c_{ex}(t)$ and $c_{ex}(t-1)$ are the CO_2 concentration in the exhaust air at the current and previous time respectively. Since the simulations are performed hourly, therefore, the mixing will be achieved between the exhaust air from the previous hour and the fresh air. For the sake of simplicity, the selected fraction f used in the current simulation is fixed

at 0.4 which was found capable of maintaining acceptable CO_2 level inside the space during the period of time lying from 12:00 till 15:00 hr.

Fig. 7 shows the effect of the proposed dehumidification strategy in decreasing the moisture content of the occupied zone between 12:00 hr. and 15:00 hr. It was found that 40% of the dry exhaust air mixed with the supply air is enough to reduce the humidity ratio, at steady conditions, from 15.3 to 13.4 g H_2O/kg of dry air between 12:00 hr and 13:00 hr, from 15.8 to 13.8 g H_2O/kg of dry air 13:00 hr and 14:00 hr, and from 16.1 to 14.1 g of H_2O/kg of dry air between 14:00 hr and 15:00 hr. Consequently, the relative humidity in the occupied zone at steady state dropped to 66.5%, 68.4% and 70% in the period 12:00-15:00 hr which is acceptable. Furthermore, the reduction in the humidity led to reinstating thermal comfort in the occupied zone at the same temperatures obtained in the base case.

It can be seen in Fig. 7 that, in the base case, the humidity ratio increased due to the elevated supply humidity ratio and then reached a steady state after 8-10 minutes of operation. The increase in the humidity on an hourly basis can be attributed to the increase in the ambient humidity and to the increment in the latent load generation within the space. In the mixed supply case, dehumidification of the DV supply air starts at 12:00 hr and this caused a sudden drop in the moisture content inside the space. Thus, the humidity of air dropped sharply and stabilized within 12 to 14 minutes. At 13:00 hr, the humidity ratio increased before stabilization. The increasing profile is due to the increased humidity ratio of the outside ambient air between 12:00 hr and 15:00 hr. It is worth mentioning that the transient period in the case of mixing 40% of the exhaust air with the fresh air is longer than the case of 100% fresh air. This is explained by the fact that mixing the exhaust air with the supply air will delay the steady state because the conditions of the air in the

occupied zone are dependent on the conditions of the exhaust air that are related in its turn to the conditions of the desiccant solution.
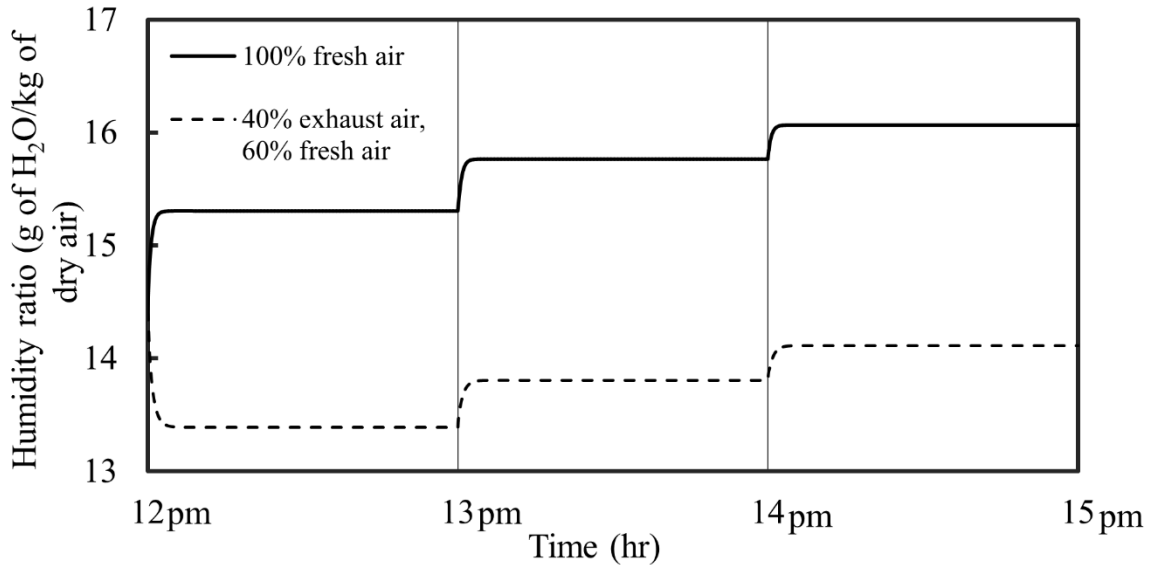
Figure 7: Variation of the humidity ratio in the occupied zone, between 12:00 and 15:00 pm with and without mixing 40% of the exhaust air with the supply; at $T_s = 20°C$, a Calcium Chloride ($CaCl_2$) solution flow rate of 0.5 kg/s and concentration of 38%

B. Economic analysis of the mixed supply dehumidification vs. conventional sub-cool and reheat dehumidification

The economic feasibility of the proposed humidity-control strategy is presented for the case study. The energy consumption of the LDMC-C/DV system with mixed supply was compared to that of a LDMC-C/DV system with conventional sub-cool and reheat dehumidification system that can attain the same DV supply air temperature and moisture content. The conventional dehumidification method involved cooling the supply air to below its dew-point temperature in order to reach the required moisture content. This was followed by reheating the air using an electric heater to meet the design supply temperature. Both systems were assumed to be equipped with the same air-to-air

exchanger (85% efficiency) that partially cooled the supply air with the exhaust air. Comparison was carried out over the 3-hour period extending from 12:00 hr to 15:00 hr when the indoor relative humidity was high and dehumidification of the supply air was required. The economic analysis was based on the energy required by the cooling coil in the mixed supply DV system as compared to the energy demand by the sub-cooling coil and electric heater in the conventional system. The difference in regeneration energy for the desiccant solution between base case and mixed strategy was neglected in the economic analysis. The reason is that the difference between the base case and adopted mixed case in the mass concentration of the liquid desiccant and the outlet desiccant temperature were less than 0.003% and 0.04ºC respectively resulting in a minimal change in the regeneration energy .

Table 3 summarizes the energy consumption of the two dehumidification systems during the period from 12:00 hr to 15:00 hr as well as the temperature and humidity ratio of the mixed air. In the conventional system, around 2.45 kWh were consumed by the sub-cooling coil and 0.22 kWh by the heating unit during three hours of operation. On the other hand, around 2.03 kWh was consumed by the system with the mixed supply which results in around 24% energy savings compared to the total 2.67 kWh consumed by the conventional system. The lower energy consumption of the LDMC-C/DV system with the proposed humidity control strategy was mainly due to the mixing with the cool dry exhaust air that rendered the supply air at a temperature close to the design temperature, which is assumed to be 20 ºC in this study. This consequently reduced the cooling load of the coil. Finally, the coefficient of performance (COP) of the system is estimated. The COP is the space cooling load of the integrated liquid desiccant membrane and DV system divided by the needed chiller electrical energy. The space cooling load is divided into the

sensible load of the DV and membrane as well as the latent load of the membrane system. The chiller work energy is determined from the cooling energy needed in both the DV (supply air sensible cooling) and the ceiling membrane system (liquid desiccant cooling) and the assumption of a typical chiller COP value of 4. During three hours of operation of the system, the total heat removed by the system was found to be 4.22 kWh and the corresponding energy demand was found to be 1.2 kWh. The resulting COP of the system was consequently found to be 3.5.

Table 3: Energy demand for the mixed supply dehumidification system and conventional dehumidification system

Hour of the day	Mixing Method			Sub-cool and Reheat Method	
	Humidity after mixing (g of H_2O/ kg of air)	Temperature after mixing (ºC)	Cooling energy (kWh)	Sub-cooling energy (kWh)	Reheating energy (kWh)
12:00-13:00	14.2	23.63	0.68	0.85	0.11
13:00-14:00	14.54	23.65	0.67	0.82	0.08
14:00-15:00	14.75	23.64	0.68	0.78	0.03
Total Energy (kWh)			2.03	2.45	0.22

C. Conclusions

The feasibility of a mixing humidity control strategy for LDMC-C/DV has been studied using validated simulation models. The strategy is based on mixing the DV fresh supply air with a fraction of the cool and relatively dry exhaust air near the ceiling. The effectiveness of the strategy was demonstrated on a case study of a typical office space. The relative humidity in the occupied zone fluctuated throughout the day and exceeded

70% during three hours of the day when the internal latent load and the outside humidity were both high. When applying the mixing strategy during the critical hours, the exhaust air mixing fraction needed to be maintained at 0.4 to keep the CO_2 concentration below the maximum allowable value. The corresponding drop in the humidity in the occupied zone resulted in reaching acceptable comfort within short period while saving energy

BIBLIOGRAPHY

A. Bahman, L. Rosario, M.M. Rahman, Analysis of energy savings in a supermarket refrigeration/HVAC system, Applied Energy. 98 (2012) 11–21. doi:10.1016/j.apenergy.2012.02.043.

A. Kabeel, Adsorption–desorption operations of multilayer desiccant packed bed for dehumidification applications, Renewable Energy. 34 (2009) 255–265. doi:10.1016/j.renene.2008.04.011.

A. Keblawi, N. Ghaddar, K. Ghali, L. Jensen, Chilled ceiling displacement ventilation design charts correlations to employ in optimized system operation for feasible load ranges, Energy and Buildings. 41 (2009) 1155–1164. doi:10.1016/j.enbuild.2009.05.009.

A. Keblawi, N. Ghaddar, K. Ghali, Model-based optimal supervisory control of chilled ceiling displacement ventilation system, Energy and Buildings. 43 (2011) 1359–1370. doi:10.1016/j.enbuild.2011.01.021.

A. Novoselac, J. Srebric, A critical review on the performance and design of combined cooled ceiling and displacement ventilation systems, Energy and Buildings. 34 (2002) 497–509. doi:10.1016/s0378-7788(01)00134-7.

A.H. Abdel-Salam, G. Ge, C.J. Simonson, Performance analysis of a membrane liquid desiccant air-conditioning system, Energy and Buildings. 62 (2013) 559–569. doi:10.1016/j.enbuild.2013.03.028.

ANSI/ASHRAE Standard 62.1-2007: ventilation for acceptable indoor air quality, American Society of Heating, Refrigerating and Air-Conditioning Engineers, Atlanta, GA, 2007.

ASTM International - Compass Login. (n.d.). https://compass.astm.org/EDIT/html_annot.cgi?D6245 12 (accessed May 26, 2018).

C.-G. Bornehag, J. Sundell, T. Sigsgaard, Dampness in buildings and health (DBH): Report from an ongoing epidemiological investigation on the association between indoor environmental factors and health effects among children in Sweden, Indoor Air. 14 (2004) 59–66. doi:10.1111/j.1600-0668.2004.00274.x.

D. Yuill, G. Yuill, A. Coward, Measurement and Analysis of Vitiation of Secondary Air in Air Distribution Systems (RP-1276), HVAC&R Research. 14 (2008) 345–357. doi:10.1080/10789669.2008.10391013.

E. Dougherty, WHY DO WE SWEAT MORE IN HIGH HUMIDITY?, (2011). http://engineering.mit.edu/ask/why-do-we-sweat-more-high-humidity (accessed March 12, 2018).

H. Schlichting, K. Gersten, Boundary layer theory, Springer, Berlin, 2000.

H. Tang, X.-H. Liu, Y. Jiang, Theoretical and experimental study of condensation rates on radiant cooling surfaces in humid air, Building and Environment. 97 (2016) 1–10. doi:10.1016/j.buildenv.2015.12.003.

H.B. Hemingson, C.J. Simonson, R.W. Besant, Steady-state performance of a run-around membrane energy exchanger (RAMEE) for a range of outdoor air conditions, International Journal of Heat and Mass Transfer. 54 (2011) 1814–1824. doi:10.1016/j.ijheatmasstransfer.2010.12.036.

H.E. Feustel, C. Stetiu, Hydronic radiant cooling — preliminary assessment, Energy and Buildings. 22 (1995) 193–205. doi:10.1016/0378-7788(95)00922-k.

J. Liu, X. Liu, T. Zhang, Performance comparison and exergy analysis of different flow types in internally-cooled liquid desiccant dehumidifiers (ICDs), Applied Thermal Engineering. 142 (2018) 278–291. doi:10.1016/j.applthermaleng.2018.07.006.

J. Miriel, L. Serres, A. Trombe, Radiant ceiling panel heating–cooling systems: experimental and simulated study of the performances, thermal comfort and energy consumptions, Applied Thermal Engineering. 22 (2002) 1861–1873. doi:10.1016/s1359-4311(02)00087-x.

J.F. Straube, Moisture in buildings, ASHRAE Journal. 44 (2002) 15.

J.W. Studak, J.L. Peterson, A Preliminary Evaluation of Alternative Liquid Desiccants for a Hybrid Desiccant Air Conditioner, in: Proceedings of the Fifth Symposium on Improving Building Systems in Hot and Humid Climates., 1988.

K. Ghali, N. Ghaddar, M. Ayoub, Chilled ceiling and displacement ventilation system for energy savings: A case study, International Journal of Energy Research. 31 (2007) 743–759. doi:10.1002/er.1266.

K. Keniar, K. Ghali, N. Ghaddar, Study of solar regenerated membrane desiccant system to control humidity and decrease energy consumption in office spaces, Applied Energy. 138 (2015) 121–132. doi:10.1016/j.apenergy.2014.10.071.

L. Zhang, J. Niu, Indoor humidity behaviors associated with decoupled cooling in hot and humid climates, Building and Environment. 38 (2003) 99–107. doi:10.1016/s0360-1323(02)00018-5.

M. Hout, N. Ghaddar, K. Ghali, N. Ismail, M. Simonetti, G.V. Fracastoro, J. Virgone, A. Zoughaib, Displacement ventilation with cooled liquid desiccant dehumidification membrane at ceiling; modeling and design charts, Energy. 139 (2017) 1003–1015. doi:10.1016/j.energy.2017.08.046.

M. Kanaan, N. Ghaddar, K. Ghali, Simplified Model of Contaminant Dispersion in Rooms Conditioned by Chilled-Ceiling Displacement Ventilation System, HVAC&R Research. 16 (2010) 765–783. doi:10.1080/10789669.2010.10390933.

M. Muslmani, N. Ghaddar, K. Ghali, Performance of combined displacement ventilation and cooled ceiling liquid desiccant membrane system in Beirut climate, Journal of Building Performance Simulation. 9 (2016) 648–662. doi:10.1080/19401493.2016.1185153.

M. Tu, C.-Q. Ren, L.-A. Zhang, J.-W. Shao, Simulation and analysis of a novel liquid desiccant air-conditioning system, Applied Thermal Engineering. 29 (2009) 2417–2425. doi:10.1016/j.applthermaleng.2008.12.006.

M.R. Abdel-Salam, M. Fauchoux, G. Ge, R.W. Besant, C.J. Simonson, Expected energy and economic benefits, and environmental impacts for liquid-to-air membrane energy exchangers (LAMEEs) in HVAC systems: A review, Applied Energy. 127 (2014) 202–218. doi:10.1016/j.apenergy.2014.04.004.

M.R. Abdel-Salam, R.W. Besant, C.J. Simonson, Design and testing of a novel 3-fluid liquid-to-air membrane energy exchanger (3-fluid LAMEE), International Journal of Heat and Mass Transfer. 92 (2016) 312–329. doi:10.1016/j.ijheatmasstransfer.2015.08.075.

M.R. Abdel-Salam, R.W. Besant, C.J. Simonson, Performance testing of a novel 3-fluid liquid-to-air membrane energy exchanger (3-fluid LAMEE) under desiccant solution regeneration operating conditions, International Journal of Heat and Mass Transfer. 95 (2016) 773–786. doi:10.1016/j.ijheatmasstransfer.2015.10.065.

M.R. Abdel-Salam, R.W. Besant, C.J. Simonson, Performance testing of 2-fluid and 3-fluid liquid-to-air membrane energy exchangers for HVAC applications in cold–dry climates, International Journal of Heat and Mass Transfer. 106 (2017) 558–569. doi:10.1016/j.ijheatmasstransfer.2016.09.024.

M.T. Fauchoux, C.J. Simonson, D.A. Torvi, P. Mukhopadhyaya, M.K. Kumaran, S.W. Dean, Tests of a Novel Ceiling Panel for Maintaining Space Relative Humidity by Moisture Transfer from an Aqueous Salt Solution, Journal of ASTM International. 6 (2009) 102034. doi:10.1520/jai102034.

Öberg V., D.Y. Goswami, Experimental Study of the Heat and Mass Transfer in a Packed Bed Liquid Desiccant Air Dehumidifier, Journal of Solar Energy Engineering. 120 (1998) 289. doi:10.1115/1.2888133.

P. Mazzei, F. Minichiello, D. Palma, HVAC dehumidification systems for thermal comfort: a critical review, Applied Thermal Engineering. 25 (2005) 677–707. doi:10.1016/j.applthermaleng.2004.07.014.

P. Nielsen, Analysis and Design of Room Air Distribution Systems, HVAC&R Research. 13 (2007) 987–997. doi:10.1080/10789669.2007.10391466.

R. Eldeeb, M. Fauchoux, C.J. Simonson, Applicability of a heat and moisture transfer panel (HAMP) for maintaining space relative humidity in an office building using TRNSYS, Energy and Buildings. 66 (2013) 338–345. doi:10.1016/j.enbuild.2013.07.021.

R. Qi, L. Lu, H. Yang, Investigation on air-conditioning load profile and energy consumption of desiccant cooling system for commercial buildings in Hong Kong, Energy and Buildings. 49 (2012) 509–518. doi:10.1016/j.enbuild.2012.02.051.

S. Cho, P. Im, J.S. Haberl, Literature review of displacement ventilation, 2005.

S.A. Mumma, Chilled Ceiling condensation control, ASHRAE IAQ Applications. (2003) 3–22.

S.B. Riffat, X. Zhao, P.S. Doherty, Review of research into and application of chilled ceilings and displacement ventilation systems in Europe, International Journal of Energy Research. 28 (2004) 257–286. doi:10.1002/er.964.

S.-M. Huang, M. Yang, X. Yang, Performance analysis of a quasi-counter flow parallel-plate membrane contactor used for liquid desiccant air dehumidification, Applied

Thermal   Engineering.   63   (2014)   323–332. doi:10.1016/j.applthermaleng.2013.11.027.

T. Imanari, T. Omori, K. Bogaki, Thermal comfort and energy consumption of the radiant ceiling panel system, Energy and Buildings. 30 (1999) 167–175. doi:10.1016/s0378-7788(98)00084-x.

W. Chakroun, K. Ghali, N. Ghaddar, Air quality in rooms conditioned by chilled ceiling and mixed displacement ventilation for energy saving, Energy and Buildings. 43 (2011) 2684–2695. doi:10.1016/j.enbuild.2011.06.019.

X. Hao, G. Zhang, Y. Chen, S. Zou, D.J. Moschandreas, A combined system of chilled ceiling, displacement ventilation and desiccant dehumidification, Building and Environment. 42 (2007) 3298–3308. doi:10.1016/j.buildenv.2006.08.020.